Colloids and Surfaces A: Physicochem. Eng. Aspects 446 (2014) 127–133

Contents lists available at ScienceDirect

Colloids and Surfaces A: Physicochemical and Engineering Aspects

journal homepage: www.elsevier.com/locate/colsurfa

# Electrocapacitive properties of supercapacitors based on hierarchical porous carbons from chestnut shell

Lulu Cheng[a,b], Peizhi Guo[a,b,*], Rongyue Wang[a,b], Lufei Ming[a,b], Fangfang Leng[a,b], Hongliang Li[a,b], X.S. Zhao[a,b,c]

[a] State Key Laboratory Breeding Base of New Fiber Materials and Modern Textile, Collaborative Innovation Center for Marine Biomass Fibers, Materials and Textiles of Shandong Province, Qingdao University, Qingdao 266071, PR China
[b] School of Chemical Science and Engineering, Qingdao University, Qingdao 266071, PR China
[c] School of Chemical Engineering, The University of Queensland, St Lucia, Brisbane QLD 4072, Australia

## HIGHLIGHTS

- Porous carbons are prepared from chestnut shells by a chemical activation method.
- The surface chemistry and surface area of porous carbons can be tuned subtly.
- The microstructure of porous carbons can be adjusted by changing the activation temperature.
- The electrocapacitive feature of porous carbons is closely related to their surface areas.

## GRAPHICAL ABSTRACT

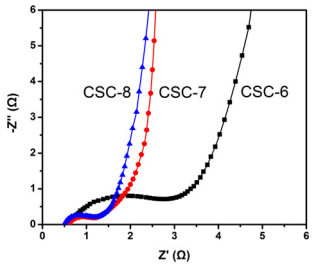


## ARTICLE INFO

*Article history:*
Received 25 August 2013
Received in revised form 12 January 2014
Accepted 15 January 2014
Available online 27 January 2014

*Keywords:*
Supercapacitor
Chestnut shell
Porous carbon
Electrode
Carbonization

## ABSTRACT

Three porous carbons CSC-6, CSC-7, and CSC-8 were prepared by the carbonization of zinc chloride-pretreated chestnut shells at 600, 700, and 800 °C under $N_2$ atmosphere and had specific surface areas of 1754, 1987, and 1824 $m^2 g^{-1}$, respectively. The microstructure and surface functional groups of samples CSCs were characterized by thermal gravimetric analysis (TGA), X-ray photoelectron spectroscopy (XPS), transmission electron microscopy (TEM) and Raman spectroscopy. Electrochemical performances of CSCs-based supercapacitors were evaluated by cyclic voltammetry (CV), galvanostatic charge–discharge, self-discharge, cycle stability, and electrochemical impedance spectroscopy (EIS) in two-electrode cells. Comparative studies showed that the CSC-7-based supercapacitor exhibited the best electrochemical performance among all the CSCs-based supercapacitors. At a current density of 0.1 A $g^{-1}$, the CSCs-based electrodes had the specific capacitances of 42.5, 105.4, and 83.4 F $g^{-1}$ in 6 M KOH solutions for CSC-6, CSC-7, and CSC-8, respectively. With the current density up to 10 A $g^{-1}$, the CSC-7-based electrode still showed a capacitance as high as 92.0 F $g^{-1}$. Based on the experimental results, the relationship between the electrochemical properties of the CSCs-based supercapacitors and structural nature of samples CSCs was analyzed and discussed.



## 1. Introduction

Supercapacitors (also called electrochemical capacitors) have received significant amount of attention, because of their extensive applications in a wide range of fields, such as mobile electronic devices and hybrid vehicles. Contrast to batteries and conventional

* Corresponding authorat: Qingdao University, School of Chemical Science and Engineering, Ningxia Road 308#, Qingdao, PR China. Tel.: +86 532 859 51290; fax: +86 532 859 55529.
*E-mail addresses:* guopz77@yahoo.com, pzguo@qdu.edu.cn (P. Guo).

0927-7757/$ – see front matter © 2014 Elsevier B.V. All rights reserved.
http://dx.doi.org/10.1016/j.colsurfa.2014.01.057

dielectric capacitors, supercapacitors have more advantages, such as environmental friendliness, long life, excellent reversibility and high power density [1–4]. Generally, supercapacitors can be divided into two types based on the modes of energy storage, electrochemical double-layer capacitors (EDLCs) and redox supercapacitors [5]. Recently, the construction of targeted supercapacitors has also been made great progress through the rational design of both the electrode materials and cell structures [6,7].

Considerable researches focused on the improvement of the electrode materials for supercapacitors have been done to increase the power density and energy density of supercapacitors [8,9]. Porous carbon has been proved to be an ideal candidate as electrode materials for supercapacitors, because of low cost, excellent conductivity, high porosity (electrolyte accessibility), and excellent chemical stability [8–10]. The energy storage mechanism of electrodes based on porous carbon mainly depends on the charge accumulation in the electrical double layers formed at the electrode/electrolyte interface, although part of the capacitance can be attributed to pseudo-faradaic reactions [5]. The surface chemistry depending on the activation conditions as well as the pore size of raw carbon materials also plays an important role in determining the electrochemical performance of carbons-based supercapacitors [11].

Supercapacitors based on porous carbons obtained by chemical activation of carbon materials can usually exhibit excellent electrochemical performance, which significantly depends on the pore size, specific surface area and surface chemistry of the porous carbons [11,12] as well as the pore wall thickness and constituting graphene layers orientation [10,13]. However, the capacitances of porous carbons are not strictly proportional to the specific surface areas, because part of the surface area is inert in the charge storage [14,15].

In this paper, porous activated carbons as the electrode materials were obtained by the carbonization of zinc chloride-pretreated chestnut shells at 600, 700, and 800 °C under $N_2$ atmosphere. Usually, porous carbons from chestnut shells have been used as adsorbents for the removal of heavy metal ions and organic pollution [16–18]. The microstructures of chestnut shell-based carbons (CSCs) were characterized by nitrogen adsorption measurements at liquid nitrogen temperature (77 K). The pore size distributions of samples CSCs were mainly micropores with microporous areas larger than 90% of the total specific surface areas. It was found that the CSC sample obtained at the temperature of 700 °C showed the highest specific surface area of 1987 $m^2 g^{-1}$ among three samples CSCs, and the CSC-7-based symmetric supercapacitors also displayed the highest electrocapacitive performance.

## 2. Experimental

### 2.1. Materials

Chestnut shells were obtained from chestnuts purchased at Qingdao market. The used chemicals purchased from Sinopharm Chemical Reagent Company included potassium hydroxide, zinc chloride, hydrochloric acid, and isopropanol. Polytetrafluoroethylene latex (PTFE, 60 wt%) was purchased from Strem Chemicals, and acetylene carbon black (99.99%) was from Aldrich. The used double distilled water was prepared in our laboratory.

### 2.2. Synthesis of the porous carbon

The mixture of water, chestnut shells, and zinc chloride with the mass ratio of chestnut shells and zinc chloride of 1:2 was dried at 80 °C. Next, the mixture was heated at 600, 700, and 800 °C for 90 min to obtain three chestnut shell-based carbons, referred as CSC-6, CSC-7, and CSC-8, respectively, in a tube furnace under nitrogen atmosphere. The heating rate was 10 °C $min^{-1}$. The three obtained solids were soaked in 5% hydrochloric acid solution for 24 h in order to remove the residual inorganic components, and then were washed with distilled water until the filtrate was neutral. Finally, the products were dried in an oven at 60 °C for 12 h.

### 2.3. Characterization of samples CSCs

The porous nature of samples CSCs was analyzed by nitrogen adsorption–desorption measurement at 77 K using ASAP 2020 Micromeritics volumetric system. The specific surface area and pore size distribution of the samples were obtained by the Brunauer–Emmette–Teller (BET) and Barrette–Joynere–Halenda (BJH) method, respectively. The micropore surface area and micropore volume were calculated by *t*-plot method. Thermal gravimetry data were collected under an air flow rate of 50 mL $min^{-1}$ on a thermogravimetric analyzer (TGA851e, Mettler Toledo), and the heating rate was 10 °C $min^{-1}$. Raman spectroscopy was performed on a Raman spectrometer (Renishaw 1000) using an $Ar^+$ laser with a 514.5 nm excitation line. X-ray photoelectron spectroscopy (XPS) measurements were carried out on an ESCALab220i-XL electron spectrometer equipped with 300 W Al Kα radiation from VG Scientific. Transmission electron microscopy (TEM) images were measured with a JEM-2000EX microscope operated at 160 kV.

### 2.4. Preparation of the CSCs-based electrodes

The electrode was prepared by mixing carbon materials (85 wt%), PTFE (5 wt%, as binder) and acetylene carbon black (10 wt%), using isopropanol as solvent. Then, the as-prepared slurry was pressed onto a nickel foam current collector (1 cm × 1 cm) at 10 MPa and dried in a vacuum oven at 110 °C. The active material mass of each electrode was about 5 mg. A symmetric supercapacitor was assembled by two electrodes separated by a porous membrane. The CSCs-based supercapacitors were abbreviated as SC-CSCs and the supercapacitors based on samples CSC-6, CSC-7, and CSC-8 were abbreviated as SC-CSC-6, SC-CSC-7, and SC-CSC-8, respectively.

### 2.5. Electrochemical measurements

Cyclic voltammetry (CV), electrochemical impedance spectroscopy (EIS), self-discharge, and galvanostatic charge–discharge technique were used to evaluate the electrochemical properties of SC-CSCs with aqueous KOH solution (6 M) as the electrolyte. A CHI760D electrochemical workstation (CH Instruments, USA) was used to perform all the electrochemical measurements.

## 3. Results and discussion

### 3.1. Sample characterization

The microstructural characteristics of samples CSCs were analyzed by nitrogen adsorption measurements. Fig. 1(A) shows the nitrogen adsorption–desorption isotherms of the CSCs. According to the IUPAC classification, the shapes of all the isotherms are close to type I (Fig. 1(A)), indicating the microporous character of these chestnut shell-based carbon materials [19,20]. Fig. 1(B) shows the pore size distributions of the CSCs, and all the CSCs have similar pore size distributions with both micropores and mesopores. The BET surface area, single point adsorption total pore volume, *t*-plot micropore area and other textural properties of samples CSCs are summarized in Table 1. The specific surface areas are 1754, 1987, and 1824 $m^2 g^{-1}$ with the total pore volumes of 0.888, 1.047, and 0.978 $cm^3 g^{-1}$ for CSC-6, CSC-7, and CSC-8, respectively. As depicted in Table 1, the micropore volume ($V_{micro}$) calculated by